Influence of low-order rational magnetic surfaces on heat transport in TJ-II heliac ECRH plasmas

2004 Nucl. Fusion 44 593

(http://iopscience.iop.org/0029-5515/44/5/003)

INSTITUTE OF PHYSICS PUBLISHING and INTERNATIONAL ATOMIC ENERGY AGENCY NUCLEAR FUSION

Nucl. Fusion **44** (2004) 593–599 PII: S0029-5515(04)77714-5

Influence of low-order rational magnetic surfaces on heat transport in TJ-II heliac ECRH plasmas

F. Castejón, D. López-Bruna, T. Estrada, E. Ascasíbar, B. Zurro and A. Baciero

Laboratorio Nacional de Fusión por Confinamiento Magnético Asociación Euratom - CIEMAT, 28040 Madrid, Spain

E-mail: francisco.castejon@ciemat.es

Received 18 November 2003, accepted for publication 15 March 2004
Published 6 April 2004
Online at stacks.iop.org/NF/44/593
DOI: 10.1088/0029-5515/44/5/003

Abstract
We study the effect of low-order rational surfaces on electron heat transport in plasmas confined in the TJ-II stellarator (Alejaldre *et al* 1990 *Fusion Technol.* **17** 131) and heated by electron cyclotron waves. Enhancement of core electron heat confinement is observed when the rational surface is placed in the vicinity of the power deposition zone, either by performing a magnetic configuration scan or by inducing Ohmic current in a single discharge. The key to improving heat confinement seems to be a locally strong positive radial electric field, which is made possible by a synergistic effect between enhanced electron heat fluxes through radial positions around low-order rationals and pump out mechanisms in the heat deposition zone.

PACS numbers: 52.25.Fi, 52.25.Xz, 52.55.Hc, 52.30.Cv

1. Introduction

An enhanced heat confinement (EHC) regime, characterized by a significant drop in core heat diffusivities, has been previously identified in TJ-II for high ECRH absorbed power density in low density plasmas [1]. The heat transport obtained from power balance is reduced as the plasma density is decreased and agrees with neoclassical estimations that take into account the effect of the electric field. A possible cause for the appearance of this regime, observed in both stellarators [2, 3] and tokamaks [4, 5], could be the interaction between ECRH and transport: microwaves push electrons into the loss cone in momentum space, enhancing their outward flux [6, 7]. The ambipolar condition for equilibrium particle fluxes ($\Gamma_e = \Gamma_i$) ensures the appearance of a positive electric field that blocks up the electron flux and reduces heat transport. This reduction is predicted by neoclassical estimations [3] and is also compatible with a reduction of turbulent transport due to sheared $E \times B$ flows [8]. The resulting electron density profile is flat or even hollow and the temperature profile is peaked. The EHC regime is due to an extended, rather than local, diminishing of heat diffusivity. The extension of the observed diminishing is $\Delta\rho \approx 0.25$, ρ being the normalized effective minor radius. A canonical definition of transport barrier cannot be found in the literature and it can be defined as a local minimum of a given transport coefficient or as a sudden increment of the corresponding gradient. The EHC regime may be associated to an electron internal transport barrier (e-ITB), since a sudden increment of temperature gradient is indeed observed. We will use the term EHC for the regime described here, but refer equivalently to the presence of an e-ITB.

Low-order rationals have been observed to reduce heat transport both in tokamaks, like RTP [9] and TEXTOR [10] (for a review on ITB formation in tokamaks see [11]), stellarators like LHD [12], where a transport barrier appears just inside a low-order rational in the plasma edge, and TJ-II, where transport reduction is observed in the edge [13] and in the plasma core [14, 15] (see [16] for a review of ITBs in stellarators). The explanation for the appearance of these barriers is still an open problem. Sheared flows can be created in the vicinity of magnetic islands [17] associated to magnetic field line resonances, and multiple transport roots can also be introduced by the presence of the island [18]. The role of rationals on stellarator transport is somehow controversial and seems to depend on their radial positions, on plasma characteristics and perhaps on magnetic shear. For instance, the effect of low-order rational surfaces has been shown to be negative for confinement in the magnetic configuration of W7-AS, when they are positioned inside the plasma column, but the best confinement windows are obtained when operating the device close to low-order resonances, including

the appearance of H-mode [19]. The presence of a resonance in the plasma edge could help in improving the confinement.

In this work, we go deeper into the study of the effect of low-order rationals on heat confinement in the core of TJ-II [15], an almost shearless, middle size flexible heliac ($R = 1.5\,\mathrm{m}$, $a < 0.22\,\mathrm{m}$) that can achieve a wide range of rotational transform values changing the currents in the central conductor coils. Together with that, a set of Ohmic coils allows us to tailor the core rotational transform profile, thus shifting low-order rationals inside the plasma in one discharge. Till now, TJ-II plasmas have been created and heated by two gyrotrons of 300 kW each, although for the discharges studied in this work only one gyrotron is used. The vacuum rotational transform profile, ι is characterized, beyond being almost flat, by a small negative shear $s = -\mathrm{d}(\ln(\iota/2\pi))/\mathrm{d}r$. Negative plasma currents tend to diminish the rotational transform while positive ones tend to increase it.

This paper is organized as follows. Section 2 shows the result of performing a configuration scan. The effect of moving the rational surface inside the plasma using the Ohmic current is presented in section 3. In section 4 we discuss the role of the electric field and the causes for heat confinement improvement, and we conclude in section 5.

2. Magnetic configuration scan

TJ-II flexibility allows us to modify the rotational transform value by changing the magnetic configuration. In this experiment, a magnetic configuration scan has been performed to investigate the effects of positioning the $m/n = 3/2$ resonance inside the plasma (m and n are the poloidal and toroidal numbers, respectively). Vacuum $\iota/2\pi$ profiles for magnetic configurations corresponding to three discharges to be discussed are plotted in figure 1. The experiment is performed on low density ECRH plasmas and the magnetic configuration is varied shot-to-shot changing the position of the 3/2 resonance while maintaining the same value of the line-averaged density ($n_\mathrm{l} \approx 0.6 \times 10^{19}\,\mathrm{m}^{-3}$). Thus, the electron temperature profiles shown in figure 2 correspond to the discharges #6978 in configuration 100_40_63, with vacuum rotational transform profile above the resonance; #6985 in configuration 100_38_62, with the vacuum resonance inside the plasma; and #6998 performed in configuration 100_36_62 with the resonance at an outer position. The configurations are identified by the currents ($\times 10\,\mathrm{kA}$) in the coils: the first figure corresponds to the central conductor, the second to the helical one and the third to the vertical field coil. Although ρ can only vary from 0 to 1, we allow this quantity to take values from -1 to +1 when data coming from electron cyclotron emission (ECE) are plotted. In this context, ρ is considered to be positive for the low field side and negative for the high field side of the sight line of the ECE diagnostic. We observe (figure 2) that discharge #6998 shows a steep core temperature gradient, in comparison with shot #6978, while shot #6985 is an intermediate case that displays both types of profiles but at different stages of the discharge. We illustrate this with the time traces of T_e for discharge #6985 in figure 3, where a clear jump (from 1.8 to 1.3 keV) of core plasma temperature is observed at $t = 1180\,\mathrm{ms}$. The rotational transform profile is only slightly modified by the

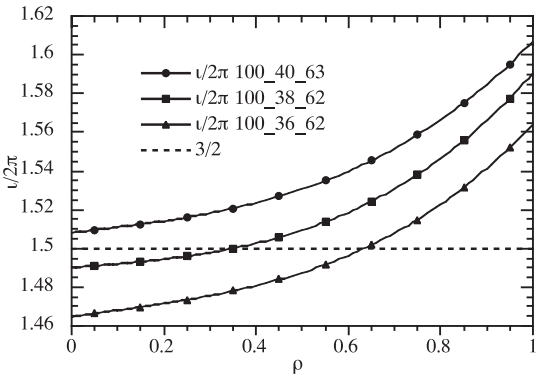

Figure 1. Vacuum rotational transform versus normalized radius for the magnetic configuration scan.

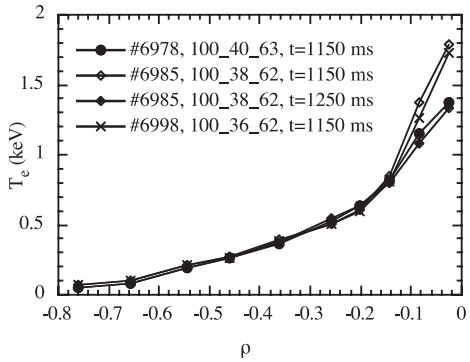

Figure 2. Temperature profiles for the magnetic configuration scan of figure 1.

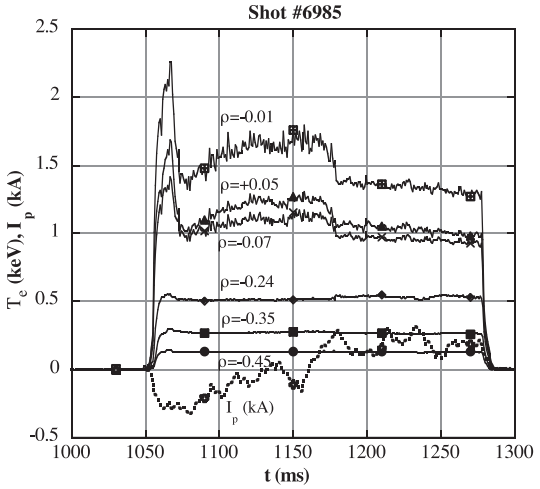

Figure 3. ECE measured temperature (identified by their normalized radius position) and bootstrap current evolution for the discharge #6985, with an intermediate value of the rotational transform.

bootstrap current [20], although its profile is unknown and very difficult to estimate accurately in TJ-II, because the total current is small in the three cases: $|I_\mathrm{p}| < 250\,\mathrm{A}$. Positive currents tend to increase the rotational transform and vice versa, but a detailed knowledge of the current density profile is necessary to elucidate the actual position of rational surfaces. This is crucial for the cases with vacuum rotational transform close to the resonance, as happens with this intermediate case. Preliminary calculations indicate that bootstrap current density

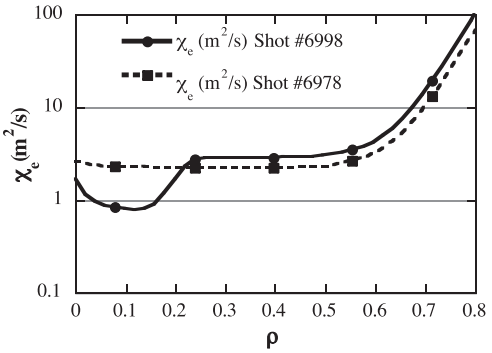

Figure 4. Heat diffusivities for the discharges #6978 and #6998.

profile is hollow, with a small positive current density near the magnetic axis, while it is negative in the plasma edge [21]. The evolution of the plasma current (see again figure 3) from small negative to small positive values in discharge #6985 (the intermediate case) can explain a slight modification (of a few cm) of the rational magnetic surface position enough to cause the disappearance of ITB. The error bar in the measurement of the plasma current is about 100 A.

The densities that correspond to this scan are very similar and so are the absorbed power densities. Therefore, the appearance of EHC or e-ITB when it happens can only be attributed to the positioning of the resonance near the plasma core. This is not the case in the EHC reported in [1], because the changes in heat confinement were observed to depend on plasma and power densities.

Transport analysis is performed using the 1.5D transport code Proctr [1]. A model based on the ISS95 scaling law [22] has been modified, as in [1], to include the enhancement of electron heat confinement in the plasma core and hence simulate these discharges. The heat diffusivity depends on plasma parameters, as the ISS95 at $\rho = 2/3$, and is diminished in the core to simulate the temperature gradient increase. The results are plotted in figure 4 showing a clear diminishing of transport in the plasma core. The core thermal diffusivities are $\chi_e \approx 2.2\,m^2\,s^{-1}$ for shot #6978 and $\chi_e \approx 1\,m^2\,s^{-1}$ for #6998, showing a significant transport reduction when the rational surface is present. The single-pass absorbed power is assumed to be $P_{ECH} = 250$ kW in both discharges, the radiated power is also the same in the two discharges, $P_{RAD} = 10\%$ of the absorbed power, and the power transferred to the ions by collisions is about $P_{ei} \approx 5\%$ of absorbed power. The power deposition profile obtained by fast modulation experiments [23] is centred, since the absorbed power density is very small (less than 10% of the maximum) for $|\rho| > 0.25$, as can be seen in figure 5. The reduction of heat diffusivity observed in the core ($|\rho| < 0.25$) of discharge #6998 is due to the presence of the steeper temperature gradient and is assumed to be due to the presence of the rational. Nevertheless, the influence on global confinement is small, around 6% and less than the error bars, since the volume inside the ITB is a small fraction of the total one. The conductivities are equal within the error bars outside e-ITB.

The average core plasma rotation speed of these discharges has been measured by spectroscopic techniques [24]. The measurements are taken during a long integration time (about 100 ms) and are radially averaged from normalized radii

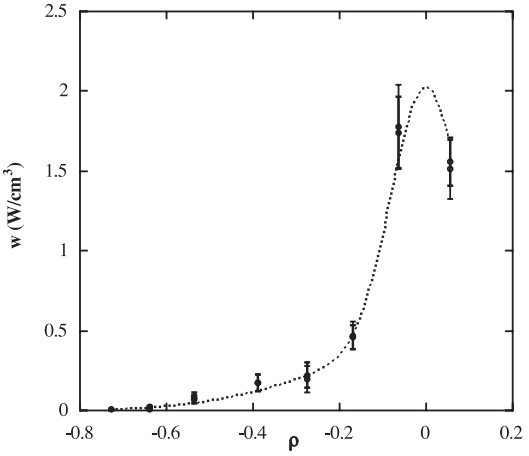

Figure 5. Power deposition profile for plasma characteristics similar to those of these experiments obtained using high frequency power modulation. The experimental points correspond to two discharges.

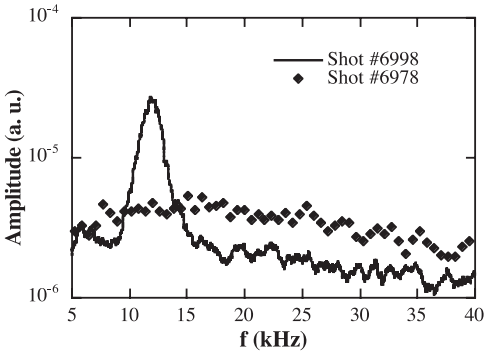

Figure 6. Fourier spectra of Mirnov coil signals corresponding to discharges #6998, with the 3/2 rational surface inside the plasma, and #6978, without the rational surface.

$\rho = -0.2$ to $\rho = 0.2$. The rotation velocity has been found to be considerably higher for EHC discharge #6998 ($\approx 7\,km\,s^{-1}$) than for the regular shot #6978 ($\approx 3\,km\,s^{-1}$). Moreover, the presence of the island inside the poloidally rotating plasma column could be detected by the Mirnov coil sets, despite the fact that they are best suited to detect modes near the plasma edge. Figure 6 shows the Fourier analysis of Mirnov coil signals for discharges #6998 and #6978 proving the existence of a coherent mode in the case with the resonance inside the plasma. The mode frequency ($\approx$12 kHz) is roughly of the order of magnitude of the expected frequency for a rotating island. A precise comparison cannot be given due to the uncertainties in the position of the resonance and the integral character of the measurements. Nevertheless, there is a link between the presence of the island near the plasma core and the enhanced core plasma rotation, which is not necessarily in contradiction with what one would expect from an increment of viscosity due to the broken magnetic geometry: the increase in the electric field due to the presence of the rational surface may overcome the stronger viscosity, thus increasing plasma rotation.

3. Effect of Ohmic current

As mentioned above, the TJ-II stellarator is equipped with a set of coils that can be used to induce an Ohmic current

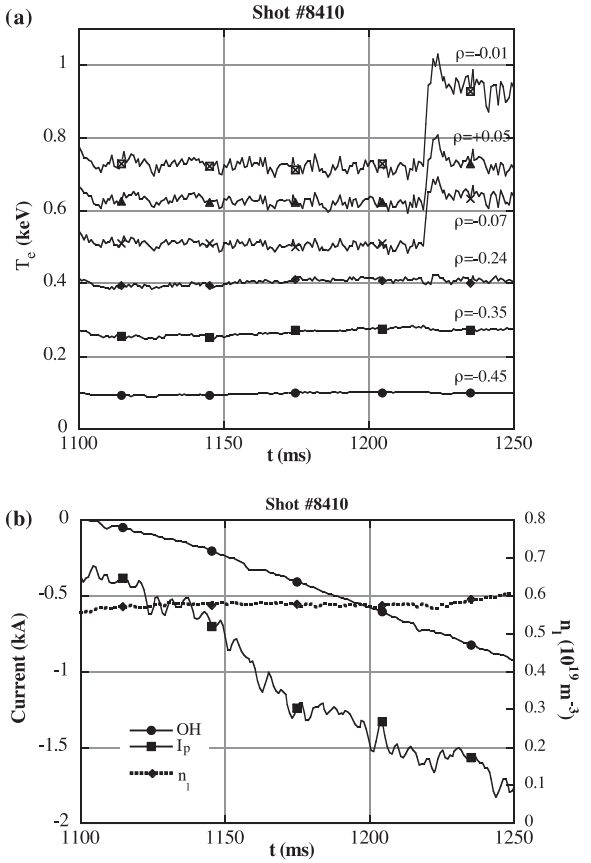

Figure 7. Time evolution of (*a*) temperature and (*b*) line density, OH coil current and plasma current for the case of Ohmic current induction.

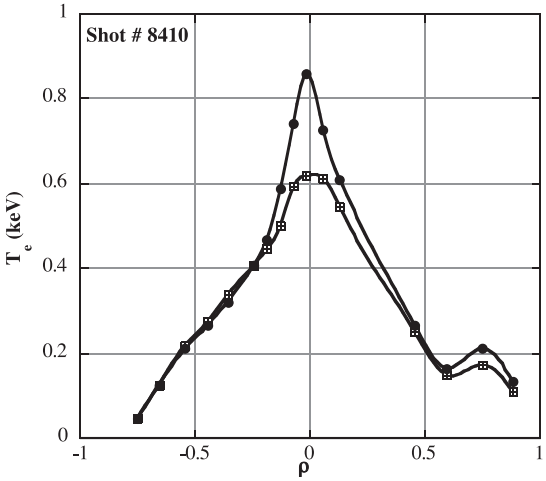

Figure 8. Temperature profiles obtained with a fit (lines) to ECE data (markers) before ($t = 1210$ ms) and after ($t = 1235$ ms) the transition. The content of superthermal electrons is very similar before and after the transition as can be seen in the three ECE channels close to $\rho = +0.8$.

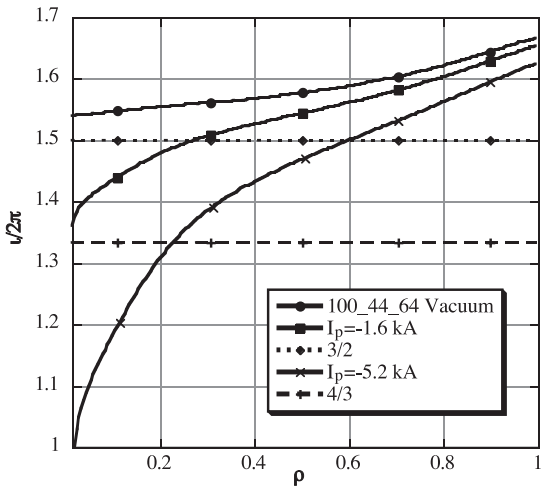

Figure 9. Vacuum and modified rotational transform profiles for $I_\mathrm{p} = -1.6$ kA and -5.2 kA. The two lowest order rationals appearing are marked for reference.

in the plasma. In this way, it is possible to change dynamically the current during the discharge and to study the effect of modifying the rotational transform profile on plasma confinement [25]. This feature gives us an extra tool to tailor the rotational transform profile and introduce low-order rationals in a controlled way, without the uncertainties of bootstrap current profile of the configuration scan. The induction process is so slow that the plasma can be considered to follow a sequence of almost steady states. Figure 7(*a*) shows the time traces of ECE channels, while figure 7(*b*) shows the line density, current in the OH coils, and net plasma current in a shot belonging to the configuration 100_44_64, whose central vacuum rotational transform satisfies $\iota(0)/2\pi = 1.55$. The central ECE channels suffer a jump for a given value of plasma current (about $I_\mathrm{p} = -1.6$ kA), showing a clear increase in heat confinement coincident with the presence of the 3/2 resonance near the plasma core. T_e profiles before and after the jump, plotted in figure 8, are similar to those corresponding, respectively, to shots #6978 and #6998 (figure 2). Note that the plasma line density does not decrease. The humps in the temperature profiles that appear at $\rho = 0.8$ correspond to downshifted emission of superthermal electrons. The foot of the steeper temperature gradient region (at $\rho \approx 0.25$; see figure 8) stays around the position, such that $\iota(r)/2\pi \approx 3/2$ once the necessary plasma current has been reached, as can be seen in figure 9. Here, we show the vacuum and a modified rotational transform profile, obtained assuming Spitzer-like resistivity corrected by the fraction of trapped particles (i.e. the current density profile satisfies $j(\rho)\,\alpha(1-f_t(\rho))\times T_\mathrm{e}^{3/2}$, being $f_t(\rho)$ the fraction of trapped particles) for $I_\mathrm{p} = -1.6$ kA, just before the transition (the ι-profile for a higher plasma current is also shown in figure 9 and we will refer to it later). The rotational transform profile has some uncertainties that can imply some modification of the position of rationals from the estimated values. First of all, there exists an experimental uncertainty in the value of the plasma current (the error bar is about 100 A); the bootstrap current still plays a role, being more important for low Ohmic currents; the presence of the current will modify the plasma equilibrium and the final rotational transform profile; finally, the rational mode will have some width that depends on the magnetic shear and mode order. It seems clear that the 3/2 surface must have come from the plasma centre but the jump in T_e does not happen until the rational surface comes to a certain outer position. It is possible that the estimate of iota profiles is not accurate enough

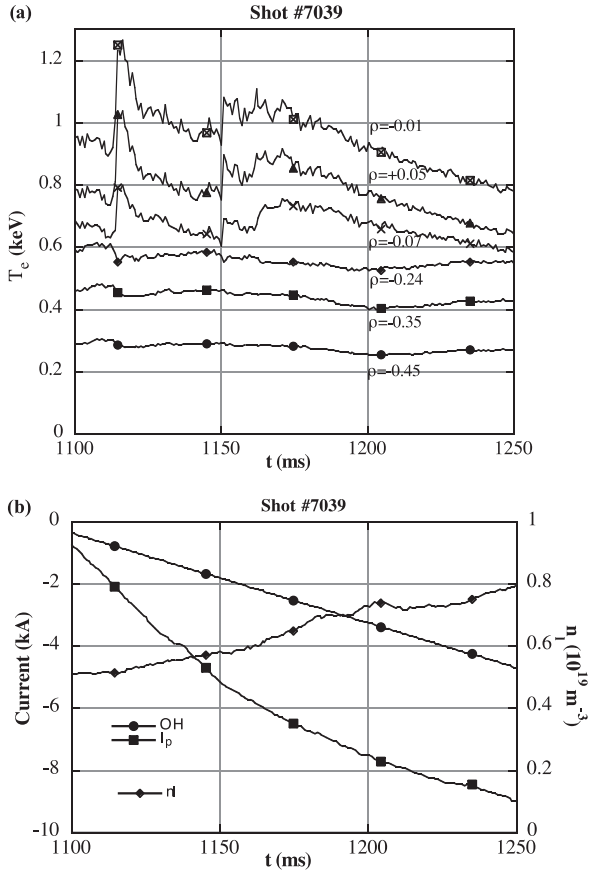

Figure 10. The same as in figures 7(*a*) and (*b*), but for shot #7039, with a stronger induced plasma current.

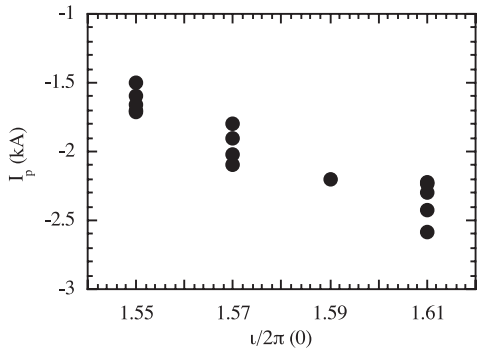

Figure 11. Values of induced plasma current needed to provoke a transition to EHC.

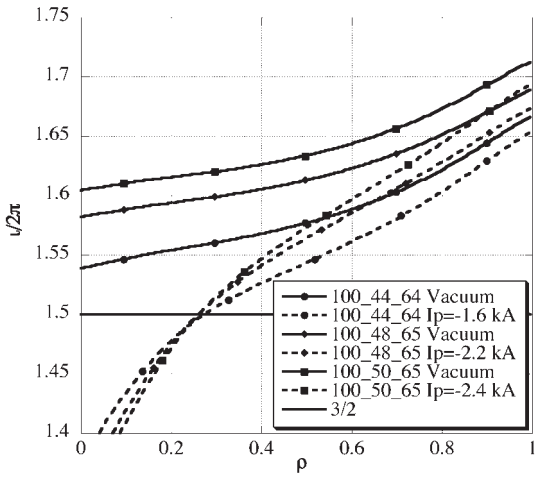

Figure 12. Vacuum and modified rotational transform profiles for the configurations of figure 11.

for the resonance to be indeed closer to the magnetic axis. On the other hand, a sort of positive feedback mechanism may be acting here: the magnetic island shows up in the plasma centre and moves out until, at some location possibly near the steepest T_e gradient, heat starts accumulating thus decreasing the resistivity and enhancing the core plasma current even further. In this way, global magnetic shear around that location narrows the effective extension of the magnetic island and the location is well defined. The trigger for such a heat accumulation will be discussed in the next section.

Larger negative currents have been induced in these plasmas. When they increase beyond a certain value it is observed that the EHC disappears as the rational surface moves further out. Figures 10(*a*) and (*b*) show the same information as figures 7(*a*) and (*b*) for discharge #7039. It can be seen that the central ECE channels suffer the jumps corresponding to the position of the 3/2 resonance near the plasma core at $I_p \approx -1.6$ kA (see figure 9). Outer channels suffer some cooling, that can also be observed in figure 7(*a*), due to a reduced transport in the core. The second transition observed at $t \approx 1150$ ms can be attributed to the appearance of the 4/3 resonance at $I_p \approx -5.2$ kA (see again figure 9). Both transitions shown in figure 10 happen in a time of the order of 1 ms and the time (20 kHz) and spatial resolution of the ECE diagnostic hardly allow us to distinguish between the starting position and propagation pattern of the transition.

These experiments show that an EHC is only triggered when the magnetic island reaches a specific location, in the vicinity of the power deposition zone. Even though ECRH driven pump-out seems to be an important ingredient for this phenomenon, as was discussed in [1], the presence of a low-order rational is required. To go deeper into this issue, Ohmic current has been induced in several magnetic configurations to provoke the appearance of the EHC. The net plasma currents needed to provoke the transition are plotted in figure 11 as a function of the central vacuum rotational transform value of the configuration (the case for $\iota(0)/2\pi = 1.55$ corresponds to the above-mentioned configuration 100_44_64). Corresponding vacuum and modified rotational transform profiles are plotted in figure 12. The farther up $\iota/2\pi(0)$ is from the 3/2 resonance, the higher the negative I_p needed to reach EHC, supporting the notion that the resonance is a necessary ingredient for this phenomenon. It is also true that the transition to EHC happens when the resonance is close to the plasma core, for normalized effective radii $\rho = 0.25$–0.3, where not only the ECH pump-out mechanism may still be at work but also the temperature gradient is the steepest.

4. The role of the electric field

What remains to be discussed now is the mechanism that starts the process of core heat accumulation. Clear contributors to the EHC have been found to be a low-order rational surface and a preferred location around the steepest temperature gradient

region. The transition to EHC has also been found to develop all of a sudden when these conditions are met. These notions will now be explained considering that the key trigger for EHC is a strong locally positive electric field [15], which can be created owing to the ambipolar condition.

The enhancement of electron flux inside the 3/2 island region is rapidly restrained by a positive electric field that also reduces collisional heat transport. The radial outward electron flux has several terms, namely the neoclassical and possible electrostatic turbulence contributions, the outward flux induced by microwaves [6, 7] and a flux due to the magnetic island that we explicitly separate:

$$\Gamma_{\rm e}(E_{\rm r}) = \Gamma_{\rm e}^{\rm NC}(E_{\rm r}) + \Gamma_{\rm e}^{\rm TURB}(E_{\rm r}) + \Gamma_{\rm e}^{\rm ECH}(E_{\rm r}) + \Gamma_{\rm e}^{\rm ISLAND}(E_{\rm r})$$

Taking into account this expression and assuming that $\Gamma_{\rm e}^{\rm TURB}(E_{\rm r})$ is automatically ambipolar (the ion and electron fluxes are equal for any electric field), several mechanisms can enhance the positive radial electric field:

(1) Low particle density for a given absorbed power density: in this case, the collisionality decreases and the neoclassical electron flux is larger than the ion one, which makes it appear that a field restores ambipolarity (electron root [26]).
(2) Increasing the absorbed power density for low collisionality: kinetic effects that tend to push particles into the loss cone, from where they are convectively removed, are eased, giving an enhanced outward electron flux [7].
(3) Positioning the resonance near the power deposition zone: it holds that $\Gamma_{\rm e}^{\rm ISLAND}(E_{\rm r}^0) \gg \Gamma_{\rm i}^{\rm ISLAND}(E_{\rm r}^0)$ ($E_{\rm r}^0$ being the electric field that is present in the plasma before the presence of the rational) so the non-ambipolar flux through the island tends to increase the positive electric field.

The first two mechanisms have already been discussed in [1] and cannot explain the results shown here. Therefore, we turn to the third mechanism, as it allows heat confinement to be improved without lowering the density for a given value of injected power.

The particle flux through a magnetic island or an ergodic zone is [27]

$$\Gamma_{\rm s} = -n_{\rm s} D_{\rm M} \left(\frac{n_{\rm s}'}{n_{\rm s}} + \frac{q_{\rm s} E_{\rm r}}{T_{\rm s}} - \frac{T_{\rm s}'}{2T_{\rm s}} \right) |v_{\rm s\parallel}| \qquad (1)$$

where $q_{\rm s}$, $v_{\rm s\parallel}$, $n_{\rm s}$ and $T_{\rm s}$ are the charge, parallel velocity, density and temperature of species s, and $D_{\rm M}$ is a geometrical coefficient that accounts for the magnetic topology. The precise calculation of these fluxes is a tough task in TJ-II. The electric field near the island created by the difference of the fluxes of ions and electrons, coming from their different thermal velocities, can be obtained with the assumption of comparatively negligible radial ion flux.

The electric field in the vicinity of the island under this assumption can be approximated by

$$E_{\rm r} \approx \frac{T}{e} \left(\frac{n'}{n} - \frac{T'}{2T} \right) \qquad (2)$$

Therefore, the steeper the background temperature gradient the stronger the field generated at the arrival of the resonance. By the way, the approximation (2) is valid for any diffusive mechanism driven by the thermodynamic force $A_1 = n_{\rm s}'/n_{\rm s} + q_{\rm s}E_{\rm r}/T_{\rm s} - T_{\rm s}'/2T_{\rm s}$, which satisfies the condition that the electron flux is much larger than the ion flux. In this way, the electric field can be estimated approximately from the temperature gradient, provided that the former approximations hold and disregarding the density gradient.

Measurements performed using HIBP confirm an increment of the radial electric field in discharges with EHC in rough agreement with equation (2) [15]. On the other hand, the electric field can be obtained from ion momentum balance considering an almost flat ion pressure profile [28]: $E_{\rm r} \approx (1/en)({\rm d}p_{\rm i}/{\rm d}r) - u_\theta B_\phi \approx -u_\theta B_\phi$. The estimate of $E_{\rm r}$ from plasma rotation measurements gives $E_{\rm r} \approx 16\,{\rm kV\,m^{-1}}$ for shot #6998 and $E_{\rm r} \approx 5\,{\rm kV\,m^{-1}}$ for shot #6978. The value of the field in the discharge showing EHC obtained using equation (2) is about $14\,{\rm kV\,m^{-1}}$, showing a rough agreement with the estimate obtained from plasma rotation.

Neoclassical transport theory predicts the appearance of multiple transport roots in stellarators and the transition between them has been observed experimentally (see, e.g. [16]). In the absence of magnetic islands and disregarding additional particle flux induced by ECRH, only a single root appears in TJ-II plasmas in the long mean-free-path regime [29]. In a recent work, the particle flux through a magnetic island is estimated in the $1/\nu$ transport regime in a tokamak [18]. Due to the presence of the island, the ambipolarity condition can yield multiple roots for the fluxes and, hence, the electric field can take several values. A mechanism of this kind could explain the EHC regime presented in this work as well as the fast transitions between enhanced and normal confinement observed in TJ-II [14, 20], although a dedicated model should be developed: the electron cyclotron heated plasmas studied are in the long mean-free-path regime and the flux through a magnetic island is much more difficult to estimate than in a tokamak. The transitions shown in this work seem to require both ingredients: pump-out and a rational surface. There still remains the question as to which mechanism is responsible for decreasing the heat transport: the modification of particle orbits by the electric field in phase space or the reduction of drift turbulence after enough $E \times B$ shear has developed. In the first case the key magnitude would be the value of the radial electric field, whereas in the second case it would be the gradient.

5. Conclusions

The effect of low rational values of rotational transform on heat transport in TJ-II plasmas has been studied by introducing them in the plasma column using two methods. First, a magnetic configuration scan was performed in TJ-II to explore the dependence of the EHC regime on configuration properties. The shapes of electron temperature profiles change along the scan and so do the transport properties. It is clearly seen that the presence of resonance near the plasma core increases the electron heat confinement in TJ-II (heat diffusivity is reduced in a factor 2).

The second method of introducing rational values inside the plasma is by inducing a toroidal plasma current in TJ-II. In this way, it is possible to change the rotational transform

profile in a controlled way and, hence, the observed enhanced electron heat confinement can only be attributed to the presence of low rational values in the discharges studied where other mechanisms can be disregarded. The arrival of the low-order rational surfaces at the high T_e gradient region favours creating a positive electric field that is able to reduce both anomalous and neoclassical transport.

Despite the uncertainties on the exact rotational transform profile cited in sections 2 and 3, both methods show that the magnetic island must approximately overlap the power deposition profile in order to reduce the heat transport. It is likely that ECRH pump-out is a cooperative mechanism in creating the necessary electric field.

The trigger that provokes the appearance of the e-ITB seems to be the electric field. The enhanced electron flux that appears when the rational surface is positioned near the plasma core creates a positive electric field. This field can be estimated assuming that ion flux is negligible compared to the electron flux; the values obtained are in agreement with the measured ones and with that estimated from plasma rotation measurements.

Acknowledgments

This work has been partially financed under project FTN2001-0688 by the Spanish 'Ministerio de ciencia y Tecnología' (Ministry of Science and Technology).

References

[1] Castejón F. *et al* 2002 *Nucl. Fusion* **42** 271
[2] Fujisawa A. *et al* 1999 *Phys. Rev. Lett.* **82** 2669
[3] Maassberg H. *et al* 2000 *Phys. Plasmas* **7** 295
[4] Pietrzyk Z.A. *et al* 2001 *Phys. Rev. Lett.* **86** 1530
[5] Buratti P. *et al* 1999 *Phys. Rev. Lett.* **82** 560
[6] Castejón F. and Eguilior S. 2003 Estimation of outward particle flux induced by ECRH *Proc. 14th Stellarator Workshop (Greifswald, Germany, September 2003)* CD-ROM
[7] Ochando M.A., Medina F. and the TJ-II Team 2003 *Plasma Phys. Control. Fusion* **45** 221
[8] Bigliari H., Diamond P.H. and Terry P.W. 1990 *Phys. Fluids* B **2** 1
[9] Lopes-Cardoso N. *et al* 1997 *Plasma Phys. Control. Fusion* **39** B303
[10] Schüller C. *et al* 2000 First results of ECRH on TEXTOR: filaments, barriers, and RI-mode *Proc. 27th EPS Conf. on Control. Fusion and Plasma Phys. (Budapest, 12–16 June 2000)* vol 24B (ECA) pp 1697–700
[11] Wolf R.C. 2003 *Plasma Phys. Control. Fusion* **45** R1
[12] Oyabu O. *et al* 2000 *Phys. Rev. Lett.* **84** 103
[13] Hidalgo C. *et al* 2000 *Plasma Phys. Control. Fusion* **42** A153
[14] Ascasíbar E. *et al* 2002 *Plasma Phys. Control. Fusion* **44** B307
[15] Estrada T. *et al* 2004 *Plasma Phys. Control. Fusion* **46** 277
[16] Fujisawa A. 2003 *Plasma Phys. Control. Fusion* **45** R1–R88
[17] García L., Carreras B.A., Lynch V.E., Pedrosa M.A. and Hidalgo C. 2001 *Phys. Plasmas* **9** 4111
[18] Shaing K.C., Hegna C.C., Callen J.D. and Houlberg W.A. 2003 *Nucl. Fusion* **43** 258
[19] Brakel R. and W7-AS team 2002 *Nucl. Fusion* **42** 903
[20] Estrada T. *et al* 2002 *Plasma Phys. Control. Fusion* **44** 1615
[21] Tribaldos V., Maassberg H., Jiménez J.A. and Varias A. 2003 *Proc. 30th EPS Conf. on Control. Fusion and Plasma Phys. (St Petersburg, 7–11 July 2003)* vol 27A (ECA) P1.28
[22] Stroth U., Murakami M., Dory R.A., Yamada H., Okamura S., Sano F. and Obiki T. 1996 *Nucl. Fusion* **36** 1063
[23] Eguilior S. *et al* 2003 *Plasma Phys. Control. Fusion* **45** 105
[24] Zurro B. *et al* 2003 *Rev. Sci. Instrum.* **74** 2056
[25] López-Bruna D., Castejón F., Estrada T., Jiménez J.A., Ascasíbar E. and Romero J.A. 2004 Effects of plasma current in the TJ-II stellarator *Nucl. Fusion* **44** at press
[26] Hastings D.E., Houlberg W.A. and Shaing K.C. 1985 *Nucl. Fusion* **25** 445
[27] Smolyakov A.I. 1993 *Plasma Phys. Control. Fusion* **35** 657
[28] Castejón F. *et al* 2003 *Rev. Sci. Instrum.* **74** 1795
[29] Tribaldos V. 2001 *Phys. Plasmas* **8** 1229